One-Way Coupling of an Atmospheric and a Hydrologic Model in Colorado

L. E. HAY

U.S. Geological Survey, Denver, Colorado

M. P. CLARK

Center for Science and Technology Policy Research, CIRES, University of Colorado, Boulder, Colorado

M. PAGOWSKI

Forecast Systems Laboratory, Cooperative Institute for Research in the Atmosphere, Boulder, Colorado

G. H. LEAVESLEY

U.S. Geological Survey, Denver, Colorado

W. J. GUTOWSKI JR.

Department of Agronomy, Geological and Atmospheric Sciences, Iowa State University, Ames, Iowa

(Manuscript received 10 January 2005, in final form 14 November 2005)

ABSTRACT

This paper examines the accuracy of high-resolution nested mesoscale model simulations of surface climate. The nesting capabilities of the atmospheric fifth-generation Pennsylvania State University (PSU)–National Center for Atmospheric Research (NCAR) Mesoscale Model (MM5) were used to create high-resolution, 5-yr climate simulations (from 1 October 1994 through 30 September 1999), starting with a coarse nest of 20 km for the western United States. During this 5-yr period, two finer-resolution nests (5 and 1.7 km) were run over the Yampa River basin in northwestern Colorado. Raw and bias-corrected daily precipitation and maximum and minimum temperature time series from the three MM5 nests were used as input to the U.S. Geological Survey's distributed hydrologic model [the Precipitation Runoff Modeling System (PRMS)] and were compared with PRMS results using measured climate station data.

The distributed capabilities of PRMS were provided by partitioning the Yampa River basin into hydrologic response units (HRUs). In addition to the classic polygon method of HRU definition, HRUs for PRMS were defined based on the three MM5 nests. This resulted in 16 datasets being tested using PRMS. The input datasets were derived using measured station data and raw and bias-corrected MM5 20-, 5-, and 1.7-km output distributed to 1) polygon HRUs and 2) 20-, 5-, and 1.7-km-gridded HRUs, respectively. Each dataset was calibrated independently, using a multiobjective, stepwise automated procedure. Final results showed a general increase in the accuracy of simulated runoff with an increase in HRU resolution. In all steps of the calibration procedure, the station-based simulations of runoff showed higher accuracy than the MM5-based simulations, although the accuracy of MM5 simulations was close to station data for the high-resolution nests. Further work is warranted in identifying the causes of the biases in MM5 local climate simulations and developing methods to remove them.

1. Introduction

Research with respect to climate simulation and prediction has attracted considerable efforts over the last 30 year, with global aspects clearly dominating. However, it is the regional and the local climate that are of central importance to societies and the biosphere. For example, a hydrologist who is interested in the water budget of a reservoir may find little help from the output of global climate models (GCMs). Even if the coarser-scale water budget would be predicted properly by the climate model, the high-resolution patterns of precipitation and temperature are of greater impor-

Corresponding author address: Dr. Lauren E. Hay, U.S. Geological Survey, Box 25046, MS 412, Denver Federal Center, Denver, CO 80225.
E-mail: lhay@usgs.gov

tance. The advent of high-resolution GCMs may improve the situation; however, hydrologic modeling at the basin scale requires climatological information on scales that are generally much finer than the typical grid size of even the highest-resolution GCMs commonly used for climate simulations (e.g., Phillips 1995). Therefore, research of "downscaling" methods has become important.

Statistical or dynamical methods can be used to downscale information from coarse-resolution GCMs to the basin scale for hydrologic modeling. Statistical downscaling (Wilks 1995; Wilby et al. 1999; McCarthy et al. 2001) uses empirical relations between features reliably simulated by a GCM at grid-box scales (e.g., 500-hPa geopotential height) and surface predictands at subgrid scales (e.g., precipitation occurrence and amounts). Dynamical downscaling uses regional climate simulations with initial and lateral boundary conditions from GCM output. This study uses regional climate simulations from the atmospheric fifth-generation Pennsylvania State University (PSU)–National Center for Atmospheric Research (NCAR) Mesoscale Model (MM5), with initial and boundary conditions from the National Centers for Environmental Prediction (NCEP)–NCAR reanalysis output (Kalnay et al. 1996), to create high-resolution (1.7-km grid spacing) climate simulations 5 years in length, centered over the Yampa River basin in northwestern Colorado.

The dramatic increase in computing power over the last few years has made it possible to run high-resolution regional climate simulations over extended periods. In a previous study, Hay et al. (2002) used daily precipitation and temperature from a 10-yr regional climate model simulation on 52-km grid spacing as input to a distributed hydrologic model for four basins in the United States. Their results indicated that the coarse resolution of the regional climate model output could be used for reliable basin-scale modeling through bias correction; but, even when bias corrected, the regional climate model output did not contain the day-to-day variability necessary for hydrologic modeling. It was felt that a finer-resolution regional climate model simulation was needed for accurate representation of precipitation and temperature at the local scale.

Grell et al. (2000) showed that high-resolution (1 km) model simulations might be necessary when the high-resolution pattern of precipitation distribution becomes important. Leung and Qian (2003) examined the sensitivity of precipitation and snowpack simulations to model resolution by nesting a regional climate model in complex terrain. A regional 40-km resolution and one 5-yr simulation at 13-km resolution for the Pacific Northwest and California were examined. They found that higher spatial resolution improves the accuracy of simulated snowpack more so than that of precipitation.

Many of the high-resolution mesoscale modeling efforts used in hydrologic applications have been conducted and analyzed for a single season or an individual storm period. For example, 1) Benoit et al. (2000) looked at one 3-day storm period in five basins in southern Ontario, Canada, using the nesting capabilities of a nonhydrostatic mesoscale atmospheric model (35-, 10-, and 3-km grid spacing) and the WATFLOOD hydrologic model; 2) Westrick and Mass (2001) looked at a 7-day rain-on-snow event in the Snowqualamie River watershed using the nesting capabilities of MM5 (36-, 12-, and 4-km grid spacing) and the Distributed Hydrology-Soil-Vegetation Model (DHSVM); 3) Westrick et al. (2002) looked at predicting peak flows during one cool season of 1998–99 over six watersheds in Washington using MM5 and DHSVM; 4) Lin et al. (2002) looked at a hydrograph during the 1996 July flash flood in the Sagenueay region of eastern Quebec, Canada, using a high-resolution atmospheric model and an offline routing module; and 5) Seuffert et al. (2002) looked at two 3-day forecasts using a mesoscale weather prediction model and the "TOPMODEL"-Based Land Surface–Atmosphere Transfer Scheme (TOPLATS)—a land surface hydrologic model.

This paper describes research that focuses on the feasibility of forecasting runoff on a daily basis over an extended period using a nonhydrostatic multiscale regional climate model at a high resolution that resolves individual valleys and massifs. To examine how well precipitation and temperature generated from a high-resolution coupled atmosphere–land surface modeling system can simulate runoff in a hydrologic model, a set of three 5-yr experiments using the nesting capabilities of MM5 was run. The first MM5 experiment was run with 20-km resolution and provided input for the higher-resolution simulations. The second and third experiments were run using 5- and 1.7-km resolutions, respectively. MM5 output was used as input to a distributed hydrologic model [U.S. Geological Survey's (USGS) Precipitation Runoff Modeling System (PRMS)] and compared with runoff produced in PRMS using standard climate observations. A multiobjective, stepwise automated technique was used to calibrate PRMS to each of the input datasets used in the comparison.

The Yampa River basin in Colorado (see Fig. 1) was chosen as the study area. The Yampa River basin is a mountainous basin where the runoff is strongly dependent on snowmelt. The basin is 1430 km^2 in area and ranges in elevation from 2000 to 3800 m. The finer-

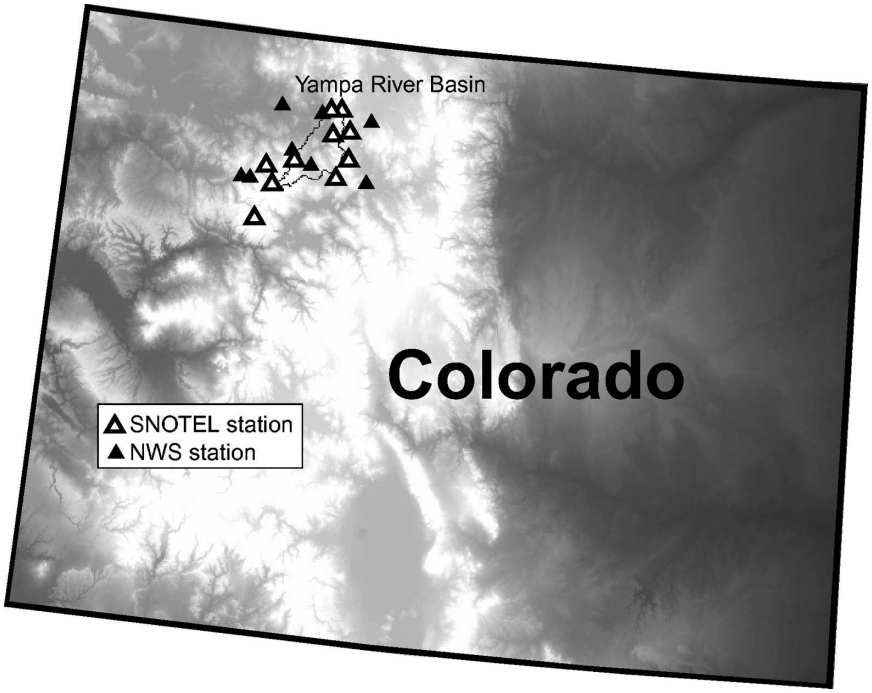

FIG. 1. Location of Yampa River basin (USGS ID 09239500) and climate stations.

resolution MM5 simulations (5 and 1.7 km) were centered over the Yampa River basin.

The strengths of this study, compared to previous high-resolution mesoscale modeling efforts, are the 1) long period of the simulations (5 years) and 2) the automated calibration of PRMS to each of the input datasets being tested (MM5 and measured climate station data). This allows for the summary of the advantages and limitations of high-resolution climate modeling with more confidence.

2. Data

The following two types of daily data were compiled for hydrologic modeling: 1) measured climate station data and 2) MM5 output.

a. Station data

Daily maximum and minimum temperature and precipitation data from stations in and around the Yampa River basin (see Fig. 1) were compiled from the National Weather Service (NWS) cooperative network of climate stations across the contiguous United States. These data were extracted from the National Climatic Data Center (NCDC) "Summary of the Day" (TD3200) dataset produced by the NOAA Climate Diagnostics Center, in Boulder, Colorado (Eischeid et al. 2000). The quality control performed by NCDC includes the procedures described by Reek et al. (1992), which flag questionable data based on checks for (a) extreme values, (b) internal consistency among the variables (e.g., maximum temperature less than minimum temperature), (c) constant temperature (e.g., five or more days with the same temperature are suspect), (d) excessive diurnal temperature range, (e) invalid relations between precipitation, snowfall, and snow depth, and (f) unusual spikes in the temperature time series. Records at most of these stations start in 1948, and continue through to the present. In addition, snow telemetry (SNOTEL) data were retrieved from the Natural Resources Conservation Service (see information available online at http:www.wcc.hrcs.usda.gov/snow). Figure 1 shows the location of the NWS and SNOTEL climate stations used in this study.

b. Atmospheric model output

A climate version of MM5 (Grell et al. 2000) was used to produce the daily precipitation and temperature inputs to PRMS. A set of three MM5 simulations were run for five water years (Wys; from 1 October 1994 through September 30 1999). These simulations were conducted using the nesting capabilities of MM5. The lateral boundary conditions produce an unavoidable negative effect on the nested simulations because of the mismatch of grid sizes, different terrain representations, and the physical parameterization's sensitiv-

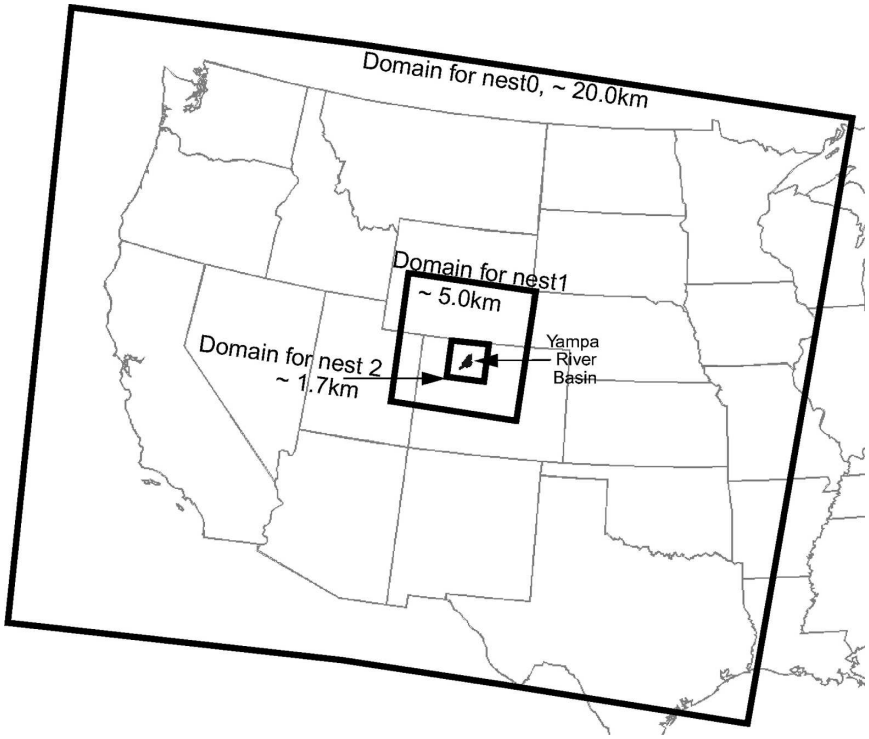

FIG. 2. Nested domains for MM5.

ity to grid size. To minimize these effects an appropriate grid-size ratio for the nested grids was chosen, and care was taken in the placement of the inner domain boundaries to avoid pronounced topographical features.

The first MM5 experiment (nest0) was run with 20-km resolution. This simulation provided input for the higher-resolution simulations. The second experiment (nest1), was centered over the Yampa River basin, and was run with 5-km resolution. The third experiment (nest2, centered over the Yampa River basin) was run with 1.7-km resolution. The size of the nest2 domain took into account the considerable computational expenses associated with the decreased integration time step to assure computational stability and to make high-resolution climate simulations feasible. Figure 2 shows the domain for each of the MM5 nests.

All precipitation is predicted explicitly when using the 1.7-km resolution (nest2), and convective parameterizations, a likely source of error (Grell et al. 2000), are excluded from the nest2 model runs. Boundary conditions for the coarse domain (nest0) came from NCEP–NCAR reanalysis output (Kalnay et al. 1996). Boundary conditions for nest1 and nest2 domains came from the nest0 and nest1 runs, respectively. The soil temperature and soil moisture were initialized by integrating nest0 and nest1 for 2 years. For nest2, initial soil temperature and moisture were interpolated from nest1 and integrated for 1 year to achieve the initial state.

The climate version of MM5 used includes all MM5 capabilities (Grell et al. 1995), such as many choices of parameterizations for convection, microphysics, radiation, and turbulence. It is also nonhydrostatic (Dudhia 1989), allowing it to be used on cloud resolving scales. Turbulence was parameterized using the 1.5-order closure developed by Burk and Thompson (1989), with the surface layer modified as in Blackadar (1976, 1979) and coupled with the land surface parameterization by Smirnova et al. (2000). This multilevel soil–vegetation scheme incorporates an energy-conserving solution for fluxes of heat and moisture in the soil and at the surface, as well as for the two-layer snow model. This model configuration was used successfully by Grell et al. (2000) in their regional climate simulations in the Alps. Also, the same coupling of the boundary layer scheme and the land surface model is used in the daily weather forecasts of the rapid uptake cycle (RUC) model (Benjamin et al. 2004) and has been evaluated on the daily basis. All of the nests employed the same parameterizations of physical processes (except for no implicit convection in nest2).

Convection was parameterized with an ensemble-based scheme (Grell and Dévényi 2002), while grid-resolved precipitation formation was parameterized us-

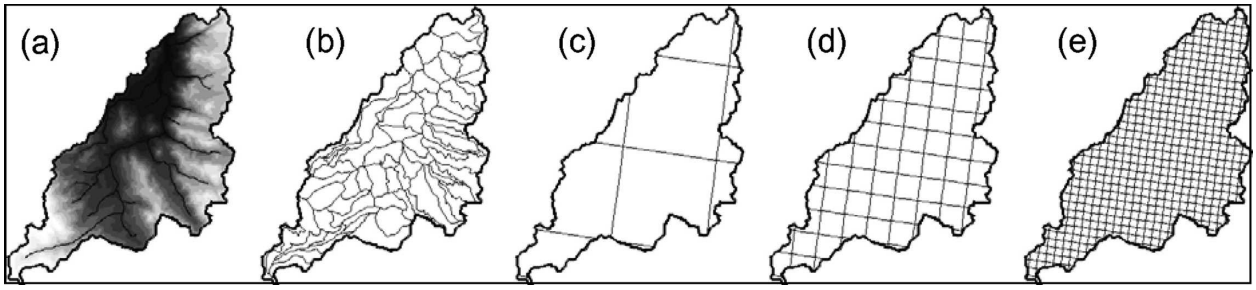

FIG. 3. Maps for the Yampa River basin showing (a) 30-m digital elevation model (DEM), (b) polygon HRU configuration, and MM5 grids at (c) 20, (d) 5, and (e) 1.7 km.

ing the Reisner scheme (Reisner et al. 1998). The Rapid Radiative Transfer Model (RRTM) scheme (Mlawer et al. 1997) was used for the parameterization of atmospheric radiation.

3. Hydrologic model

The hydrologic model chosen for this study is the U.S. Geological Survey's PRMS (Leavesley et al. 1983; Leavesley and Stannard 1995). PRMS is a distributed-parameter physically based watershed model. Distributed-parameter capabilities are provided by partitioning the watershed into hydrologic response units (HRUs). Each HRU is assumed homogenous with respect to its hydrologic response. PRMS is conceptualized as a series of reservoirs (impervious zone, soil zone, subsurface, and groundwater) whose outputs combine to produce streamflow. For each HRU, a water balance is computed daily and an energy balance is computed twice each day. The sum of the water balances of each HRU, weighted by unit area, produces the daily watershed response.

a. HRU configurations

HRU delineation, characterization, and parameterization were done using the Geographic Information System (GIS) interface the GIS Weasel (Viger et al. 1998). For this study, two types of HRUs were delineated for the Yampa River basin (see Fig. 3): 1) classic polygons and 2) grids. Climate station and MM5 output are used as input to PRMS configured with each of these HRU configurations (Figs. 3b–e).

HRUs were delineated for the polygon method by 1) subdividing the basin into two flow planes for each channel, 2) subdividing the basin using three equal area elevation bands, and 3) intersecting the flow-plane map with the elevation-band map. This resulted in 68 HRUs for the Yampa River basin (see Fig. 3b).

HRUs were delineated for the grid method based on the three MM5 nests of 1) 20-, 2) 5-, and 3) 1.7-km grids. This resulted in 11, 75, and 553 gridded HRUs for the Yampa River basin, respectively (see Figs. 3c–e).

Hydrologic model parameters describing topographic, vegetation, and soil characteristics were generated using the GIS Weasel for each HRU from the following four digital databases: 1) USGS 3-arc second digital elevation models, 2) State Soils Geographic (STATSGO) 1-km gridded soil data (U.S. Department of Agriculture 1994), 3) U.S. Forest Service 1-km gridded vegetation type and density data (U.S. Department of Agriculture 1992, personal communication), and 4) USGS 1-km gridded land use/land cover data (Anderson et al. 1976). For cases in which an HRU contained more than one soil or vegetation type, the dominant soil or vegetation type was used.

b. PRMS input datasets

For each HRU, PRMS requires daily inputs of precipitation (PRCP), maximum temperature (TMAX), and minimum temperature (TMIN). Sixteen runs were configured for PRMS and are outlined in Table 1 and Fig. 4. The runs compare 1) two types of climate input (climate stations and MM5 output), 2) two types of HRU configurations (polygons and grid cells), and 3) three methods of climate distribution (xyz; percent area, and MM5). The xyz distribution methodology is described below. The percent area method is used to compare MM5 output using the classic polygon approach of the HRU configuration with grid-cell HRU configuration. Output from the MM5 simulations were already distributed to each of the respective gridded HRU configurations (1-to-1 distribution technique in Table 1).

The xyz method uses multiple linear regressions (MLR) to distribute daily measured precipitation and maximum and minimum temperature data from a group of stations (a single daily mean value) to each HRU in a basin (Hay et al. 2000; Hay and Clark 2003)

TABLE 1. PRMS simulation name descriptions. Percent area: percent area of grid cell within each polygon; 1 to 1: no distribution needed.

PRMS simulation name	HRU configuration	Input data	Distribution to HRU method
XYZ_poly	Polygon	Station data	xyz
XYZ_20km	20 km	Station data	xyz
XYZ_5km	5 km	Station data	xyz
XYZ_1.7km	1.7 km	Station data	xyz
nest0_20km	20 km	Raw MM5 nest0	1 to 1
nest1_5km	5 km	Raw MM5 nest1	1 to 1
nest2_1.7km	1.7 km	Raw MM5 nest2	1 to 1
nest0_poly	Polygon	Raw MM5 nest0	Percent area
nest1_poly	Polygon	Raw MM5 nest1	Percent area
nest2_poly	Polygon	Raw MM5 nest2	Percent area
nest0b_20km	20 km	Bias-corrected MM5 nest0	1 to 1
nest1b_5km	5 km	Bias-corrected MM5 nest1	1 to 1
nest2b_1.7km	1.7 km	Bias-corrected MM5 nest2	1 to 1
nest0b_poly	Polygon	Bias-corrected MM5 nest0	Percent area
nest1b_poly	Polygon	Bias-corrected MM5 nest1	Percent area
nest2b_poly	Polygon	Bias-corrected MM5 nest2	Percent area

based on the longitude (x), latitude (y), and elevation (z) of the HRU. To account for seasonal climate variations, MLR Eq. (1) was developed for each month and for each dependent variable [the climate variables (CV): PRCP, TMAX, and TMIN] using the set of independent variables of x, y, and z (xyz) from the set of climate stations shown in Fig. 1,

$$\mathrm{CV} = b_1 x + b_2 y + b_3 z + b_0. \quad (1)$$

The monthly MLR equations describe the spatial relations between the monthly dependent CV and the independent xyz variables. Equation (1) describes a plane in three-dimensional space with "slopes" b_1, b_2, and b_3 intersecting the CV axis at b_0. Note that for each month the best MLR equation for a given CV did not always include all the independent variables (i.e., x, y, and z).

To estimate the daily value of each CV for each

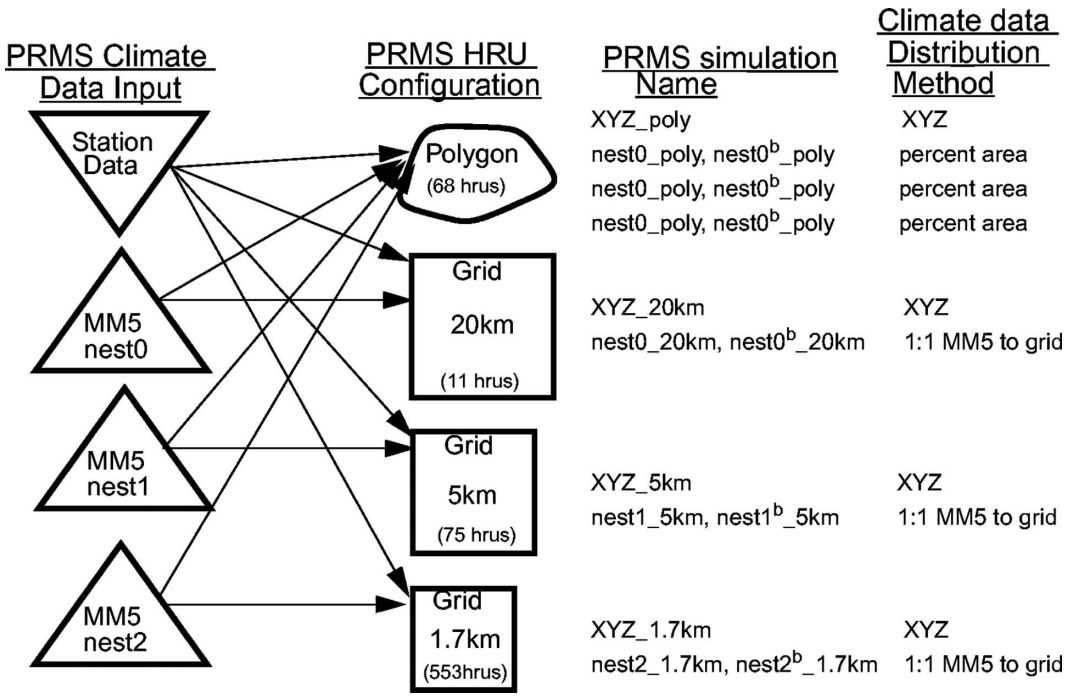

FIG. 4. Description of PRMS configurations.

TABLE 2. PRMS calibration information.

Step	Calibration dataset associated with PRMS state	PRMS parameters used to calibrate model state	Parameter description
1	Mean monthly solar radiation	dday_intcp	Intercept in temperature degree-day relation
		dday_slope	Slope in temperature degree-day relation
		tmax_index	Index temperature used to determine precipitation adjustments to solar radiation
2	Mean monthly PET	jh_coef	Coefficient used in Jensen–Haise PET computations
3	Annual water balance	adjust_rain	Precipitation adjust factor for rain days
		adjust_snow	Precipitation adjust factor for snow days
4	Daily flow components:	adjmix_rain	Factor to adjust rain proportion in mixed rain–snow event
	1) peak flow	tmax_allrain	If HRU maximum temperature exceed this value, precipitation assumed rain
	2) groundwater flow	cecn_coef	Convection condensation energy coefficient
	3) all daily flow	emis_noppt	Emissivity of air on days without precipitation
		freeh2o_cap	Free-water holding capacity of snowpack
		potet_sublim	Proportion of PET that is sublimated from snow surface
		smidx_coef	Coefficient in nonlinear surface runoff contributing area algorithm
		smidx_exp	Exponent in nonlinear surface runoff contribution area algorithm
		gwflow_coef	Groundwater-routing coefficient
		ssrcoef_sq	Coefficient to route subsurface storage to streamflow
		soil2gw_max	Maximum rate of soil water excess moving to groundwater
		soil_moist_max	Maximum available water holding capacity of soil profile
		soil_rechr_max	Maximum available water holding capacity for soil recharge zone

HRU, the following procedure was used: 1) from a set of stations, mean daily values of each CV [$CV_{(stamean)}$] and corresponding mean x, y, and z values [$x_{(stamean)}$, $y_{(stamean)}$, and $z_{(stamean)}$] were used with the slopes of the monthly MLRs in Eq. (1) to estimate a unique y intercept ($b_0$est) for that day [Eq. (2)]; and 2) Eq. (3) was solved using b_1, b_2, and b_3 from Eq. (1), $b_0$est from Eq. (2), and the x, y, and z values of the HRU of interest [$x_{(HRU)}$, $y_{(HRU)}$, and $z_{(HRU)}$],

$$b_0\text{est} = \text{CV}_{(\text{stamean})} - [b_1\, x_{(\text{stamean})} + b_2\, y_{(\text{stamean})} + b_3\, z_{(\text{stamean})}], \quad (2)$$

$$\text{CV}_{(\text{HRU})} = b_0\text{est} + b_1\, x_{(\text{HRU})} + b_2\, y_{(\text{HRU})} + b_3\, z_{(\text{HRU})}. \quad (3)$$

c. Hydrologic model calibration

To effectively assess the performance of the MM5-based simulations of runoff a multiobjective, stepwise automated calibration scheme was used (Hay et al. 2006) to calibrate PRMS using each of the input datasets (shown in Fig. 4 and Table 1), giving each type of input an "equal" performance chance. For each step in the automated calibration procedure the following were selected: 1) calibration dataset(s), 2) PRMS parameters that influence a given model state and corresponding parameter ranges, 3) objective function(s), and 4) the optimization algorithm. Table 2 lists for each calibration step the associated model state and the parameters being calibrated and their descriptions.

Calibration datasets were developed for the following four PRMS model outputs: 1) solar radiation (SR), 2) potential evapotranspiration (PET), 3) annual water balance, and 4) daily runoff components. For each model output, a single-parameter sensitivity analysis was conducted using Monte Carlo techniques. The sensitive parameters influencing each of the model outputs were calibrated in a multistep procedure similar to that presented by Hogue et al. (2000). The PRMS parameters calibrated for each model state are listed in Table 2.

The first step in the calibration procedure used mean monthly solar radiation values. The snowmelt and evapotranspiration computations in PRMS require daily values of SR. For this study, daily SR values were calculated in PRMS from daily air temperature (Leavesley et al. 1983). Where available, daily SR can be input directly into PRMS, but in general, these data are not available.

Measured monthly SR values are available for 217 stations in the United States (available online at http://rredc.nrel.gov/solar/old_data/nsrdb/redbook/mon2/). A dataset of mean monthly SR values at each of the climate station sites (SNOTEL and NWS) in the United States was developed. A MLR was developed between the measured monthly SR values at the 217 stations and independent variables (climate statistics calculated using climate stations collocated with the measured solar

radiation). For each month a separate MLR equation was developed, choosing from the following independent variables: latitude; longitude; elevation; mean precipitation (days > 0°C); mean precipitation; number of rain days; mean maximum temperature; and the difference between mean maximum and mean minimum temperature. Adjusted R^2 values ranged from 0.83 to 0.98. Mean monthly SR values, referred to as "measured" values in this paper, were calculated at each SNOTEL and NWS climate station site using the monthly MLR equations. Solar radiation output from the station closest to the centroid of the Yampa River basin was used as the calibration dataset for the first step in the calibration process.

The objective function used to calibrate the mean monthly solar radiation values produced from PRMS was as follows:

$$\text{OFabs} = \sum_{m=1}^{12} \text{abs}[\log(\text{INT}_m) - \log(\text{SIM}_m)], \quad (4)$$

where OFabs is the objective function, m is the month, and INT and SIM are the mean monthly interpolated and simulated solar radiation values, respectively.

The second step in the calibration procedure used a calibration dataset derived from mean monthly PET maps provided by the NWS. The NWS derived the PET map values from the free-water evaporation atlas of Farnsworth et al. (1982). The basin mean monthly values, referred to as measured values in this paper, were calculated from the PET maps and used in the calibration process. The objective function is similar to that used for solar radiation [Eq. (4)].

The third step of the calibration procedure used an annual water balance objective function based on the annual runoff totals,

$$\text{OFwb} = \sum_{y=1}^{\text{nyr}} \text{abs}[(\text{MSD}_y - \text{SIM}_y)/\text{MSD}_y], \quad (5)$$

where OFwb is the annual water balance objective function, y is the year, nyr is the total number of years, and MSD and SIM are the annual runoff totals for measured and simulated runoff, respectively.

The fourth step of the calibration procedure used the sum of three objective functions to calibrate daily runoff values,

$$\text{OFro} = \text{OFdaily} + \text{OFpeak} + \text{OFgw}, \quad (6)$$

where OFro is the total of three objective functions: OFdaily, OFpeak, and OFgw. OFdaily is an objective function calculated using daily measured and simulated flow values; OFpeak is an objective function calculated using daily flows that were determined to be peak values; OFgw is an objective function calculated using the groundwater portion of the daily measured and simulated flows. The groundwater portion of daily measured and simulated flows was estimated using the Hydrograph Separation (HYSEP) program of Sloto and Crouse (1996).

OFdaily, OFpeak, and OFgw were calculated using the normalized root-mean-square error (NRMSE)

$$\text{NRMSE} = \left[\sum_{n=1}^{\text{ndays}} (\text{MSD}_n - \text{SIM}_n)^2 \Big/ \sum_{n=1}^{\text{ndays}} (\text{MSD}_n - \text{MN})^2 \right]^{1/2}, \quad (7)$$

where n is the day; ndays is the total number of days; and MSD, SIM, and MN are the measured, simulated, and mean daily values associated with OFdaily, OFpeak, or OFgw.

For this study, the shuffle complex evolution (SCE; Duan et al. 1992, 1993, 1994) was chosen as the optimization algorithm. The SCE method has been used successfully by a number of researchers (e.g., Yapo et al. 1996; Kuczera 1997; Hogue et al. 2000; Madsen 2003; Hay et al. 2006), and is discussed in detail in Duan et al. (1992, 1993, 1994).

An important component of this study was to treat the MM5 output the same as the climate station data. PRMS was calibrated for each input dataset with the same technique to avoid biasing one data input over another. There were only 5 years of MM5 output for this study. Therefore, calibration had to be confined to a shorter period of time than what is usually deemed appropriate. Yapo et al. (1996) found that approximately 8 yr of data were needed to achieve model calibrations that are insensitive to the period selected. Because this was impossible for this study (only 5 years of MM5 output), it was decided to make two separate calibration runs of 2 years for each set: 1) two wet water years (WYs 1998–99) and 2) two dry water years (WYs 1996–97).

4. Results

a. Hydrologic model input data

For comparison purposes, PRCP, TMAX, and TMIN station data were distributed to each of the three MM5 nests (see Figs. 3c–e) using the xyz methodology described earlier. These xyz values at each HRU configuration were used for direct (one to one) comparison with corresponding MM5 output.

1) PRECIPITATION

Figures 5a–c shows the xyz daily basin PRCP mean by month, and that produced by MM5 for the three

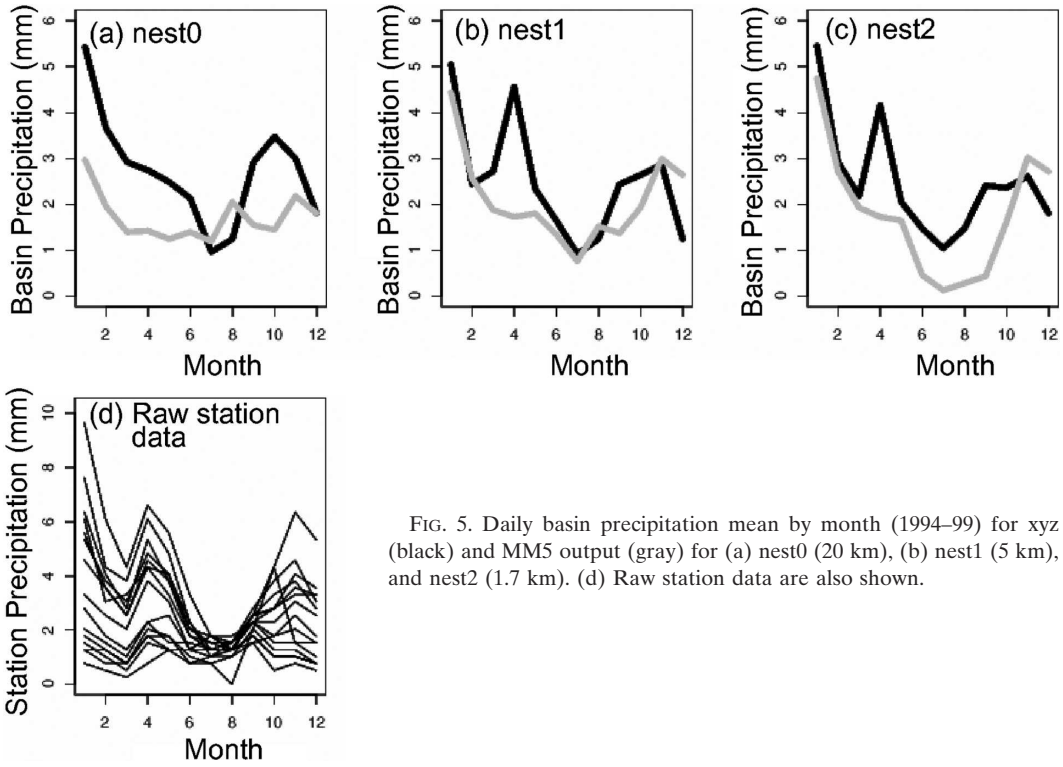

FIG. 5. Daily basin precipitation mean by month (1994–99) for xyz (black) and MM5 output (gray) for (a) nest0 (20 km), (b) nest1 (5 km), and nest2 (1.7 km). (d) Raw station data are also shown.

nests. Figure 6 shows the corresponding percent number of rain days for each by month [MM5 values below the trace value reported by climate stations (0.01 in.) were considered dry days]. The MM5 output captures the gross aspects of the seasonal cycle of the daily basin PRCP mean by month seen in the xyz output for each nest, although there are some large discrepancies. Figure 5d shows the measured daily basin PRCP mean by month for each individual climate station. The peak in PRCP mean data for the month of April that appears in the xyz nest1 and nest2 (black lines in Figs. 5b,c) is present in the station data (Fig. 5d). MM5 output (gray lines) does not show the April increase in PRCP. When compared with xyz, MM5 tends to generate more rain days but less rain (except in summer) at the coarser resolutions (nest0 and nest1, Figs. 6a–b). Rain days for MM5 are most consistent with that produced using xyz for the 5-km nest (nest1, Fig. 6b). Most notable differences are found in Fig. 6c in which MM5 produces far fewer rainy days in the summer months when compared

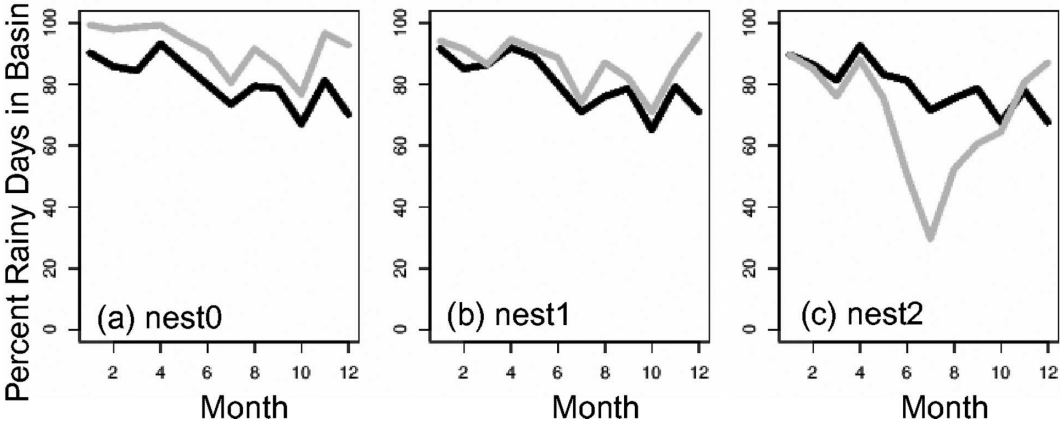

FIG. 6. Percent number of rain days by month for xyz (black) and MM5 output (gray) for (a) nest0 (20 km), (b) nest1 (5 km), and nest2 (1.7 km).

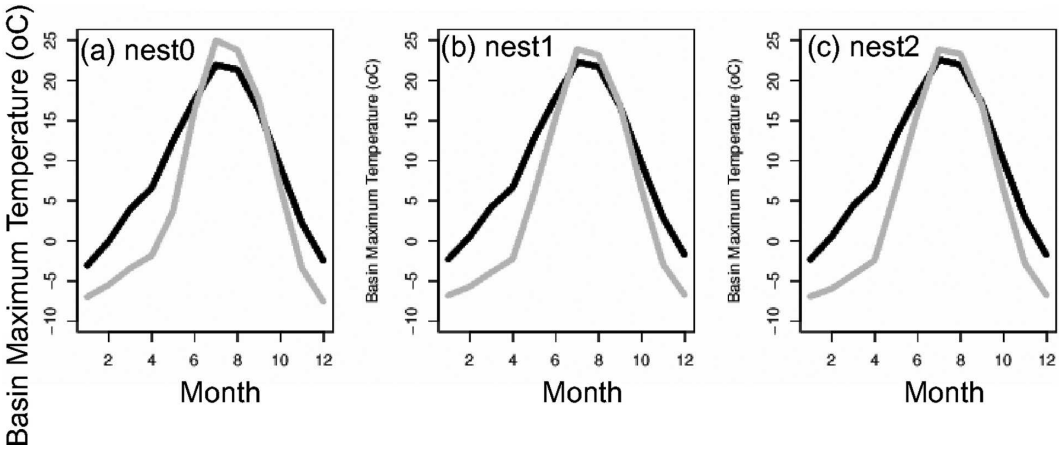

FIG. 7. Daily basin maximum temperature mean by month for xyz (black) and MM5 output (gray) for (a) nest0 (20 km), (b) nest1 (5 km), and nest2 (1.7 km).

with any of the other outputs. This translates into substantially lower summer PRCP amounts for the summer months (Fig. 5c).

Based on these results, the raw MM5 datasets were "corrected" for biases based on the xyz output for each MM5 nest. The method is similar to the transform method suggested by Panofsky and Brier (1968), and has been used by Wood et al. (2002) and Hay et al. (2002) to correct biases in the atmospheric model output that is being used in hydrologic models. The bias corrections were made on a monthly basis using a probability-swap method, which preserved the precipitation distribution. The MM5 PRCP biases were corrected using the following steps. 1) Force the MM5 PRCP values to have the same number of PRCP days as that of the xyz output. This was accomplished by (a) ranking the MM5 precipitation output and (b) setting all values to zero with ranks equal to or lower than the number of dry days in the xyz output. 2) Fit a gamma distribution to the resultant station and MM5 time series (restricted to PRCP days). 3) For each MM5 PRCP day [i.e., all MM5 values above the thresholds identified in step (1b)], compute the cumulative probability in the gamma distribution fitted to the MM5 output, and then replace the raw MM5 value with the PRCP amount associated with the matched cumulative probability in the gamma distribution fitted to the xyz output. The bias adjustments to the MM5 PRCP "correct" the monthly mean values making them identical (not shown) to that shown for the xyz in Figs. 5 and 6.

2) TEMPERATURE

Figures 7 and 8 show the xyz daily basin TMAX and TMIN mean by month (black lines) and those produced

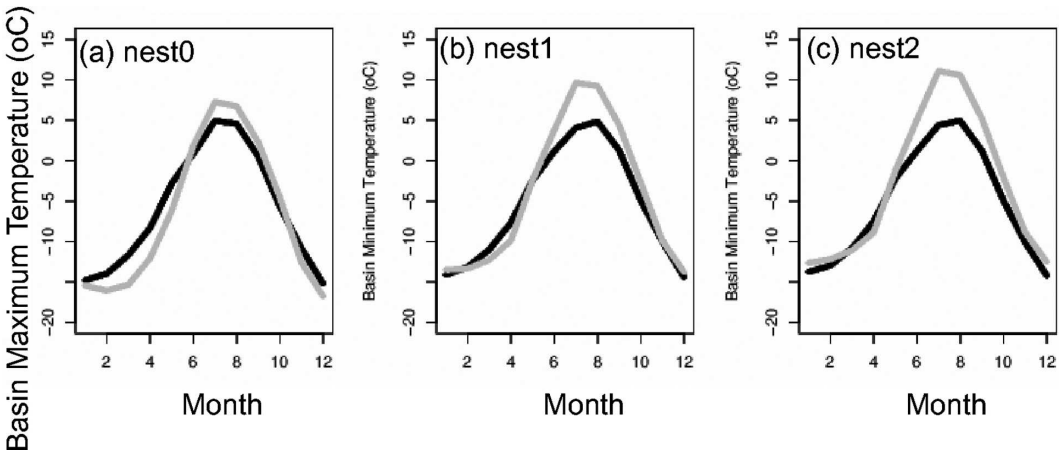

FIG. 8. Daily basin minimum temperature mean by month for xyz (black) and MM5 output (gray) for (a) nest0 (20 km), (b) nest1 (5 km), and nest2 (1.7 km).

by MM5 (gray lines) for the three nests. MM5 TMAX values are substantially lower than xyz output in all but the summer months. MM5 TMIN values are somewhat similar to xyz values in the winter months for the two finer-scale nests (Figs. 8b–c). MM5 values for all nests tend to be higher in the summer months, and for TMIN this tendency increases as the grid resolution increases.

Hay et al. (2002) found that in the snowmelt-dominated basins, PRMS simulations of runoff were strongly affected by TMAX. Based on the results for temperature shown in Figs. 7 and 8, a bias correction was performed on the raw MM5 TMAX and TMIN datasets to produce the bias-corrected MM5 temperature datasets. Biases were removed in the MM5 temperature datasets by 1) computing a monthly climatology of the MM5 maximum and minimum temperature for each day, 2) subtracting the daily MM5 value of maximum and minimum temperature from that climatology (to produce a daily anomaly value), and 3) adding the daily maximum and minimum temperature anomaly from the MM5 model to the corresponding xyz monthly station climatology of maximum and minimum temperature. Because of the nature of the temperature bias correction, the monthly climatologies of bias-corrected MM5 outputs are the same.

b. Hydrologic model output

The hydrologic model PRMS was calibrated for two calibration periods, 16 times, using three types of data (station data and raw and bias-corrected MM5 output), and four HRU configurations (polygons and 10-, 5-, and 1.7-km grids). Table 1 lists each configuration combination and the abbreviation used for each. Outputs from the following four hydrologic model states were calibrated: 1) solar radiation, 2) PET, 3) annual water balance, and 4) daily runoff components. The following sections describe the results from each calibration step.

1) SOLAR RADIATION

Figure 9 shows the basin mean monthly solar radiation values for measured versus calibrated and evaluated solar radiation values from the 16 PRMS simulations (listed in Table 1). The solid red and black lines show the results from the first step of the multistep calibration procedure. The red lines show the results using parameters calibrated using WYs 1996–97, and the black lines show the results using parameters calibrated using WYs 1998–99. The general trend for all PRMS simulations is the close match of calibrated solar radiation with that measured (gray line). Evaluated results (dashed red and black lines) for each calibration period represent the solar radiation values calculated by PRMS for the evaluation period after the final step in the multistep calibration process. The solar radiation values calculated for the two evaluation periods shows the tightest fit to that measured when using xyz-based input to PRMS.

For this study, solar radiation was estimated in PRMS using daily air temperature data (Leavesley et al. 1983). The green line in Figs. 9e–g shows the solar radiation from MM5 for comparison purposes. Mean monthly solar radiation values from MM5 match measured values in all months, except for July and August in which MM5 produces more solar radiation than that indicated in the measured data.

2) POTENTIAL EVAPOTRANSPIRATION

Figure 10 shows the basin mean monthly PET-estimated values for measured versus calibrated and evaluated PET values from the 16 PRMS simulations listed in Table 1. The solid red and black lines show the results from the second step of the multistep calibration procedure. These plots are similar to those shown for solar radiation (Fig. 9). Calibration fit is not as tight as that for solar radiation. As with solar radiation results, the PET values calculated for the two evaluation periods shows the tightest fit to measured PET when using xyz-based input to PRMS.

3) ANNUAL WATER BALANCE

An annual water balance objective function was used to calibrate annual runoff volumes. Figure 11 shows the annual water balance values for measured (gray line) versus calibrated (large gray diamonds and black dots) and evaluated (small gray diamonds and black dots) water balance values from the 16 PRMS simulations listed in Table 1. The calibration results for the annual water balance all closely match measured values, with a few exceptions when using raw MM5 input (Figs. 11e,g,k,m). Evaluation results show a consistent underestimation of the annual water balance when using the xyz-based input to PRMS. Evaluation results using MM5 output are variable.

4) DAILY RUNOFF

Three objective functions were used when calibrating the daily runoff (see Table 2). Each was computed from the daily hydrograph values, and therefore all three were calibrated in the same calibration step. Figure 12 shows results for the groundwater component of the calibration. Figure 12 is similar to that shown for the

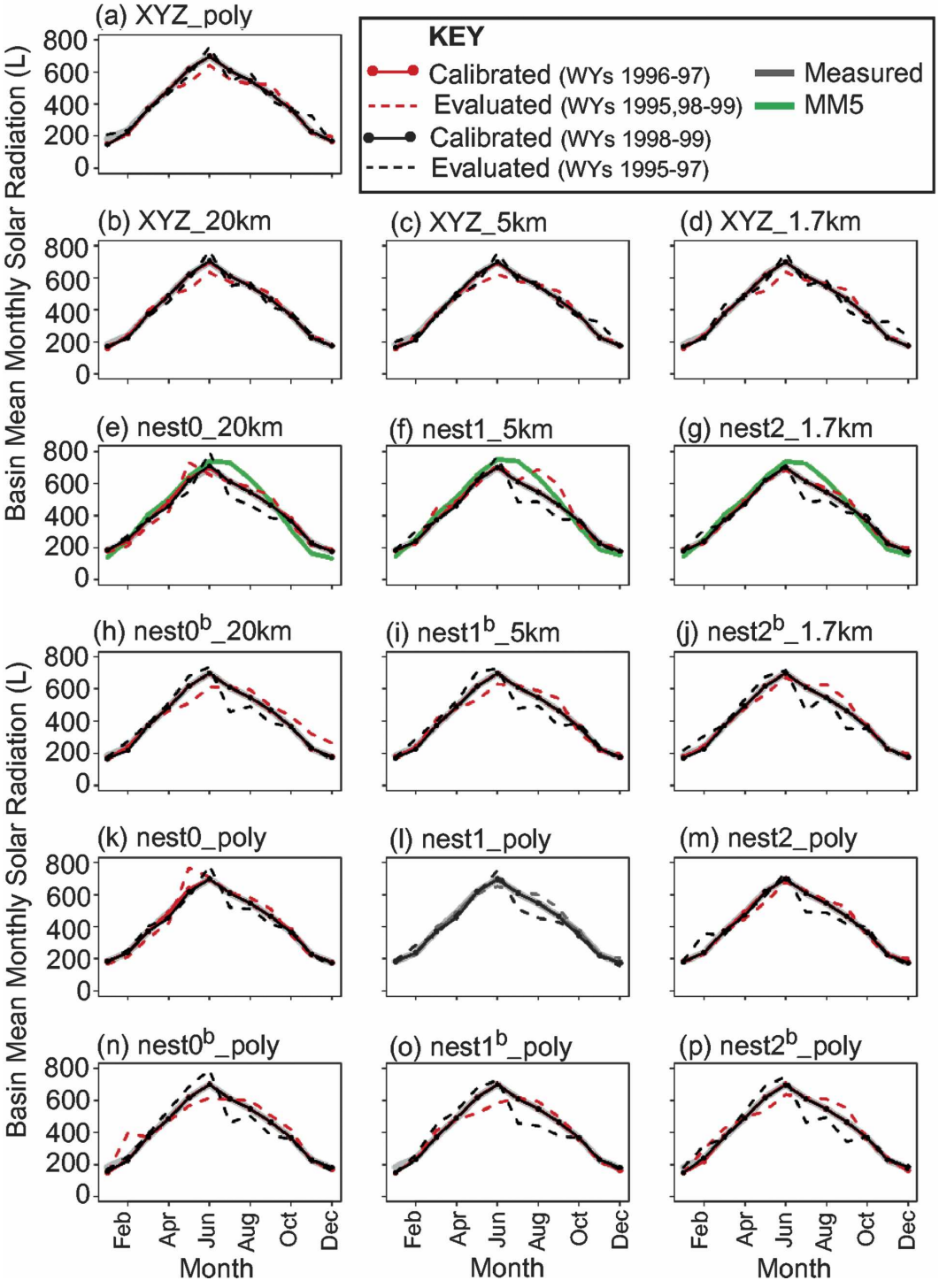

FIG. 9. Basin mean monthly solar radiation values: measured vs calibrated and evaluated values from the 16 PRMS simulations.

annual water balance (Fig. 11). In general, the calibration and evaluation results using xyz-based input to PRMS (Figs. 12a–d) all produce groundwater percentages similar to that measured. MM5 output is not nearly as consistent, although both raw and bias-corrected MM5 output distributed to the polygon HRUs produce much better estimates of groundwater than those using the MM5 grids as HRUs.

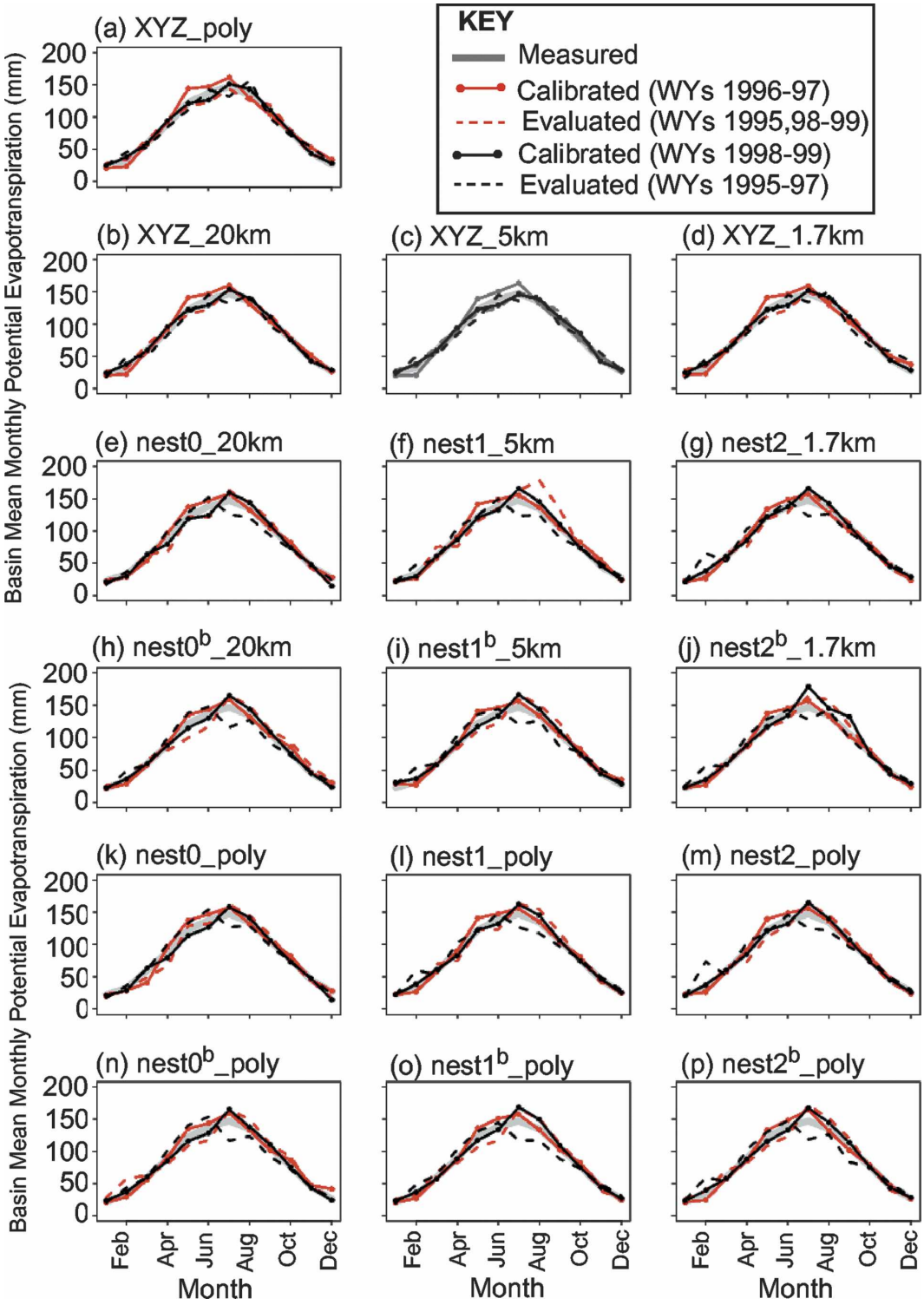

FIG. 10. Basin mean monthly potential evapotranspiration values: measured vs calibrated and evaluated values from the 16 PRMS simulations.

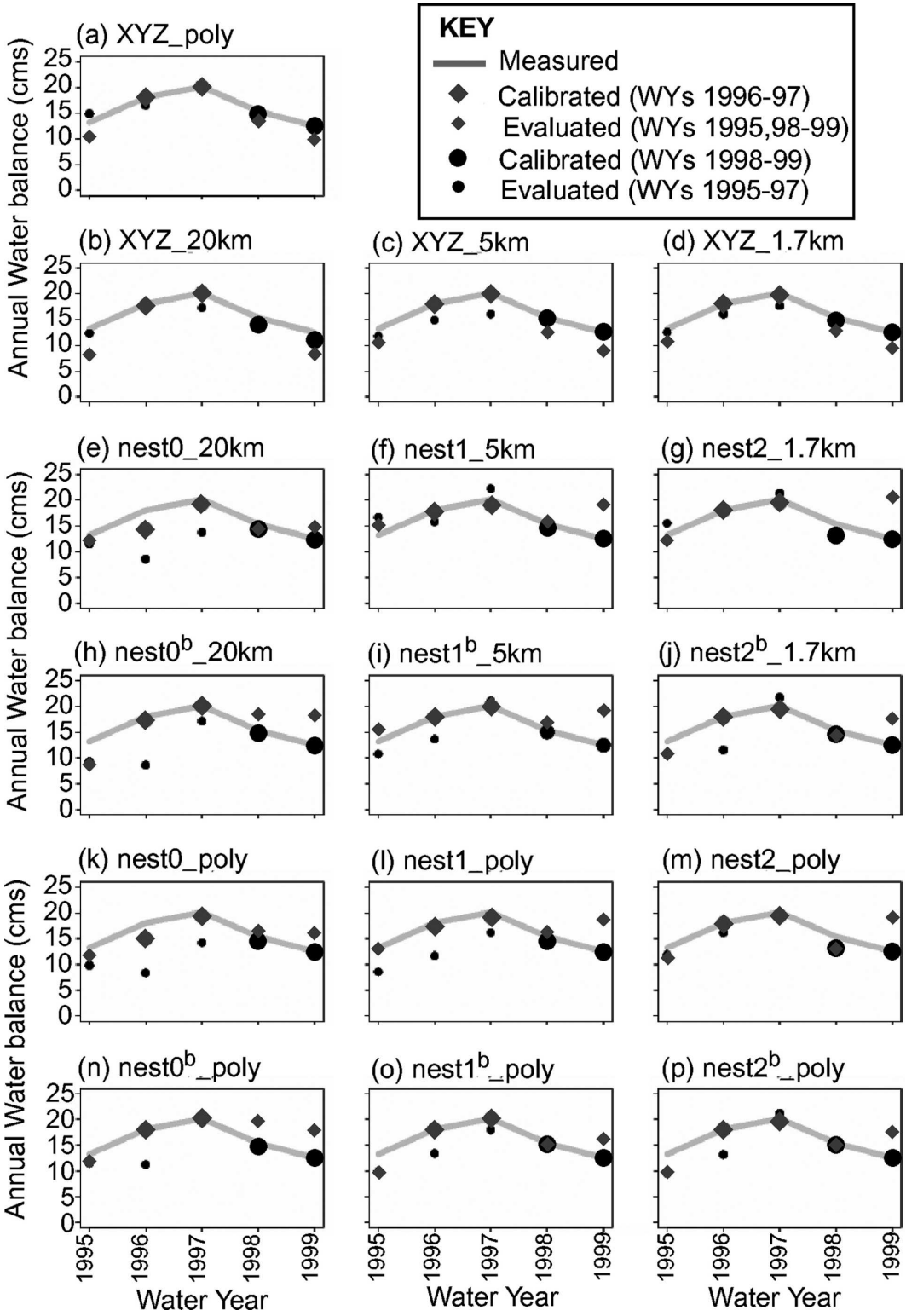

FIG. 11. Annual water balance: measured vs calibrated and evaluated values from the 16 PRMS simulations.

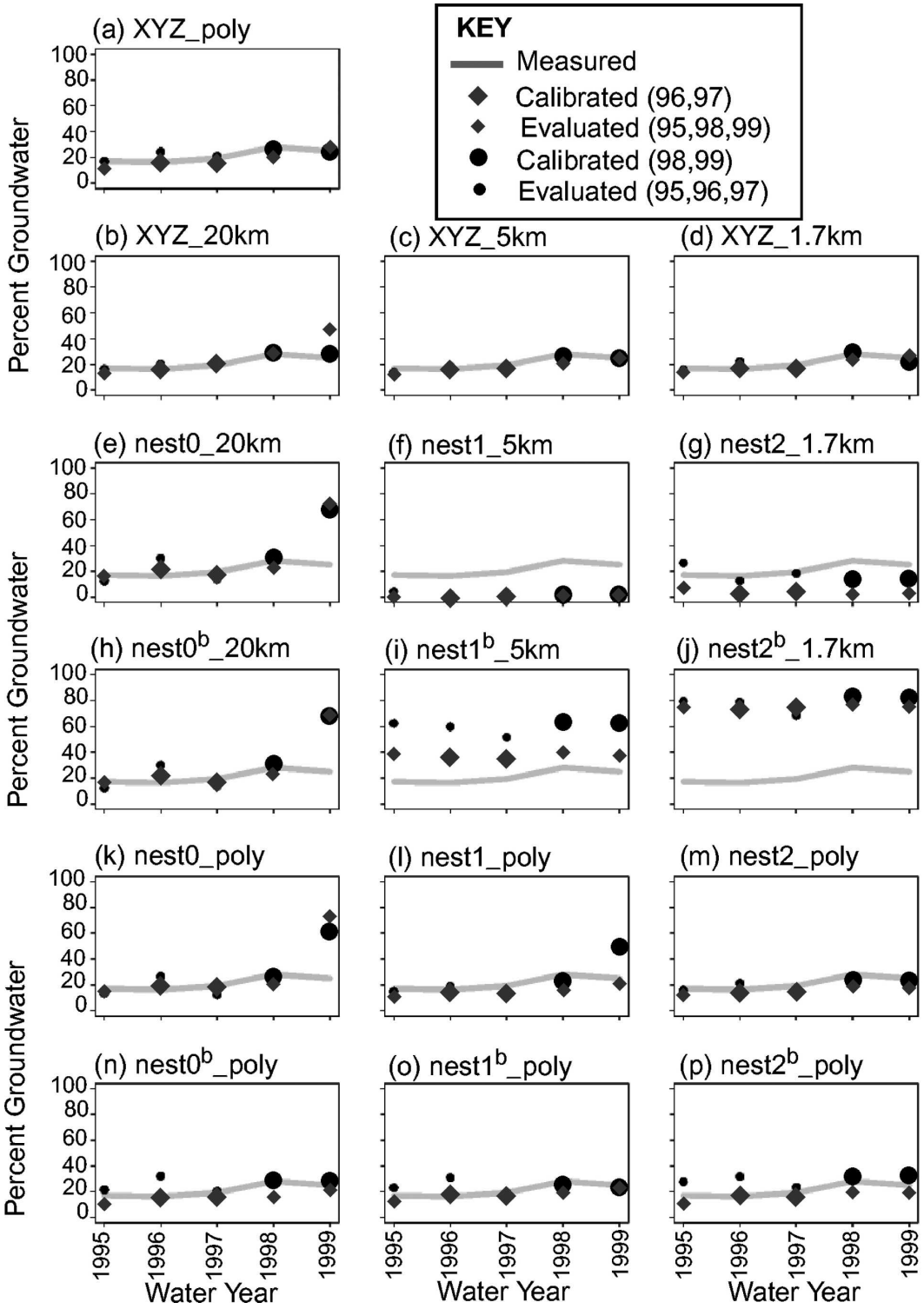

FIG. 12. Percent groundwater by year: measured vs calibrated and evaluated values from the 16 PRMS simulations.

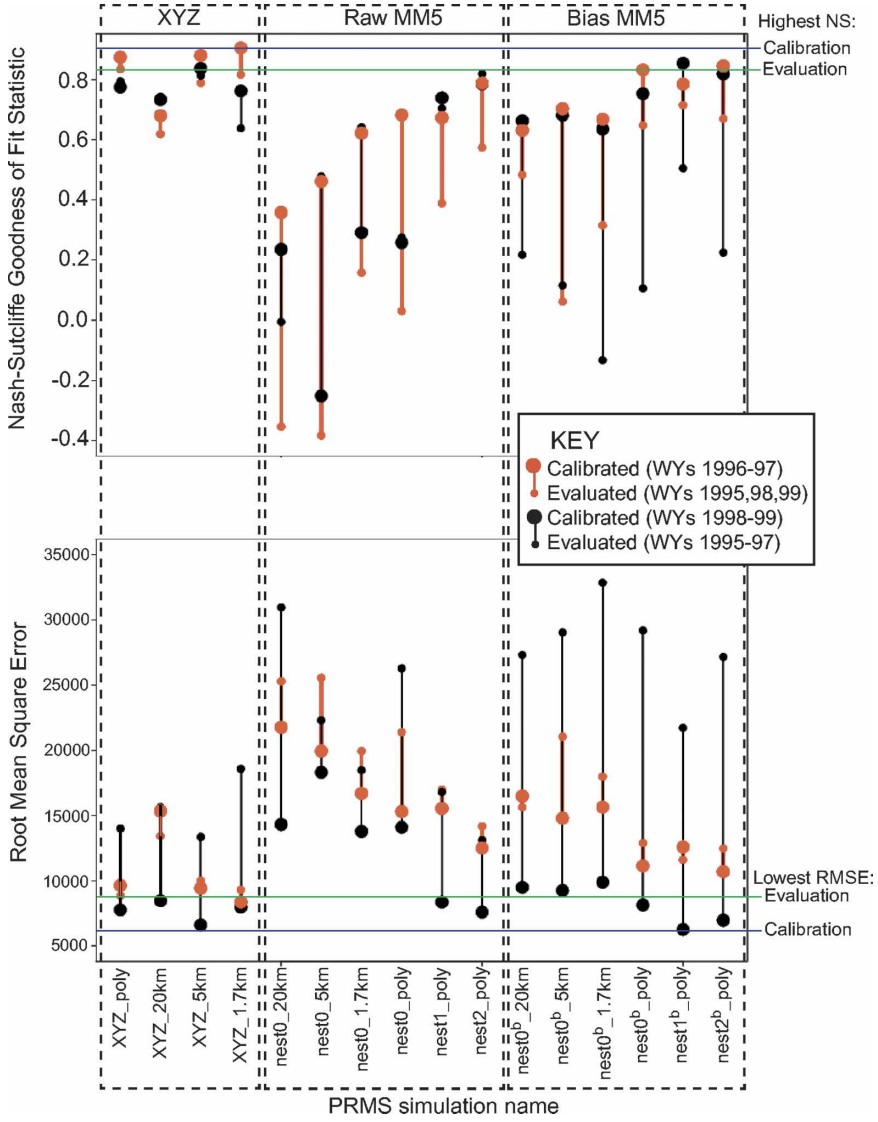

FIG. 13. Nash–Sutcliffe goodness-of-fit and root-mean-square error statistics for the two calibration/evaluation periods from the 16 PRMS simulations.

The Nash–Sutcliffe (NS) goodness of fit (Nash and Sutcliffe 1970) and the root-mean-square error (RMSE) were chosen to evaluate the performance of the PRMS calibration and evaluation for daily runoff. The NS value is calculated as follows:

$$\mathrm{NS} = 1.0 - \sum_{n=1}^{\mathrm{ndays}} (\mathrm{MSD}_n - \mathrm{SIM}_n)^2 \Big/ \sum_{n=1}^{\mathrm{ndays}} (\mathrm{MSD}_n - \mathrm{MN})^2, \tag{8}$$

where MSD is the measured daily runoff value, SIM is the simulated daily runoff values, MN is the average of the measured values, and n is the number of values out of a total of ndays. An NS value of one indicates a perfect fit between measured and simulated values. A value of zero indicates that the fit is as good as using the average value of all of the measured data.

Figure 13 shows the NS and RMSE statistics for the calibration and evaluation periods from the 16 PRMS simulations outlined in Table 1. The large red and black dots show the calibrated values and the small red and black dots show the evaluated values of the two statistics. Red indicates calibration using data for WYs 1996–97, and black indicates calibration using data for WYs 1998–99. A line is drawn between the calibrated and evaluated values for each PRMS simulation to indicate the range between the calibration and evaluation values (smaller ranges indicate better model performance).

The blue (green) horizontal line indicates the best calibration (evaluation) results for the NS and RMSE results.

Evident from Fig. 13 is the small-range and good statistic values (higher NS and lower RMSE) compared to MM5 for the xyz-based PRMS simulations, especially when calibrating using WYs 1996–97 (wet years). This is shown by the small range in the NS, and especially the RMSE. The range between the calibration and evaluation for the NS and RMSE statistics are smaller when using the wet years compared to the dry years for all PRMS simulations, with the exception of the NS values for raw MM5 output. These results agree with previous calibration studies that indicate that results are better for wet periods than for dry periods (i.e., Yapo et al. 1996).

Of particular interest in Fig. 13 is the high skill of both the raw and bias-corrected MM5 simulations. This skill is most evident for the finer nests, in which the NS scores and the RMSE are close to those obtained using station data. The high skill in the raw MM5 simulations indicates that the calibration process is able to remove the MM5 model biases.

The difference in model accuracy between calibration and evaluation is larger in the MM5 output than in the xyz station-based simulations. This is most likely a problem of "overfitting" during the calibration process, a problem that is exacerbated when using imperfect model forcing data (as is the case with the MM5 simulations). Either longer calibration periods or probabilistic methods of model calibration (e.g., Vrugt et al. 2003) may help to alleviate this problem.

Figure 14 shows scatterplots of daily runoff values produced from the 16 PRMS simulations versus the measured values from both calibration (gray dots) and evaluation (black dots) periods. The gray line indicates the one-to-one relation between simulated and measured daily runoff. The NS values for the calibration and evaluation periods on each plot are shown in gray and black, respectively.

Visual inspection of the scatterplots leads to the conclusion that the PRMS simulation using the XYZ_1.7km dataset, calibrated using WYs 1996–97, produces the most accurate runoff. The NS values for this run are very similar to those shown for the XYZ_5km- and XYZ_poly-based PRMS simulations. Consistent with what was shown in the annual water balance plots (Fig. 11), xyz-based PRMS simulations seem to show a general underestimation of the peak runoff values, but they also show much less scatter around the one-to-one line than do the MM5-based runs. For example, while the RMSE and NS values for nest2_poly or nest1^{b}_poly may look reasonable (see Fig. 13), the scatterplots in Fig. 14 show variability in the simulated flow that is not present in the measured runoff or in the xyz-based runs.

Results comparing PRMS output using polygon-based HRUs versus grid-based HRUs (see Fig. 3) generally show an increase in accuracy as resolution increases, especially when using xyz-based input to PRMS (see Fig. 13). Note that the polygon-based HRUs are approximately equal in size to the 5-km HRUs (68 versus 75 HRUs, respectively), but the PRMS output using polygon HRUs tends to have results as good as those produced using the 5- and 1.7-km HRUs (see Fig. 13). This indicates that the concept of a hydrologic response unit is a valid one, but if the HRUs are small enough, improvements in simulation accuracy may not occur. When the HRUs are increased from 5 (75 HRUs) to 1.7 (553 HRUs) km, the increase in computer run time is significant.

5. Summary and conclusions

This paper examined the simulation of runoff through coupling of a high-resolution nested mesoscale climate model and a hydrologic model. The nesting capabilities of the atmospheric fifth-generation Pennsylvania State University–National Center for Atmospheric Research Mesoscale Model (MM5) were used to create high-resolution, 5-yr-long climate simulations, starting with a coarse nest of 20 km over the western United States. During this 5-yr period two finer-resolution simulations (5 and 1.7 km) were created for the Yampa River basin in Colorado. Daily precipitation (PRCP) and maximum and minimum temperature (TMAX and TMIN, respectively) time series from the three MM5 nests (raw and bias corrected) were used as input to the U.S. Geological Survey's distributed hydrologic model [the Precipitation Runoff Modeling System (PRMS)] and compared with results using standard climate observations.

Analysis of the MM5-generated PRCP showed problems when using the 1.7-km resolution MM5 nest (nest2). The nest2 MM5 runs do not include the convective parameterizations found in the nest0 and nest1 runs, because convective precipitation should occur without parameterization at this scale (1.7 km). The nest2 MM5 runs show an underestimation of PRCP for the summer months, when convection is dominant. This has little effect on the PRMS simulations because the Yampa River basin is snowmelt dominated and summer rainfall has little impact on the hydrograph.

Analysis of the MM5-generated TMAX and TMIN indicates that errors in nest0 (20 km) are seen in nest1 (5 km) and nest2 (1.7 km). The finer-resolution nests

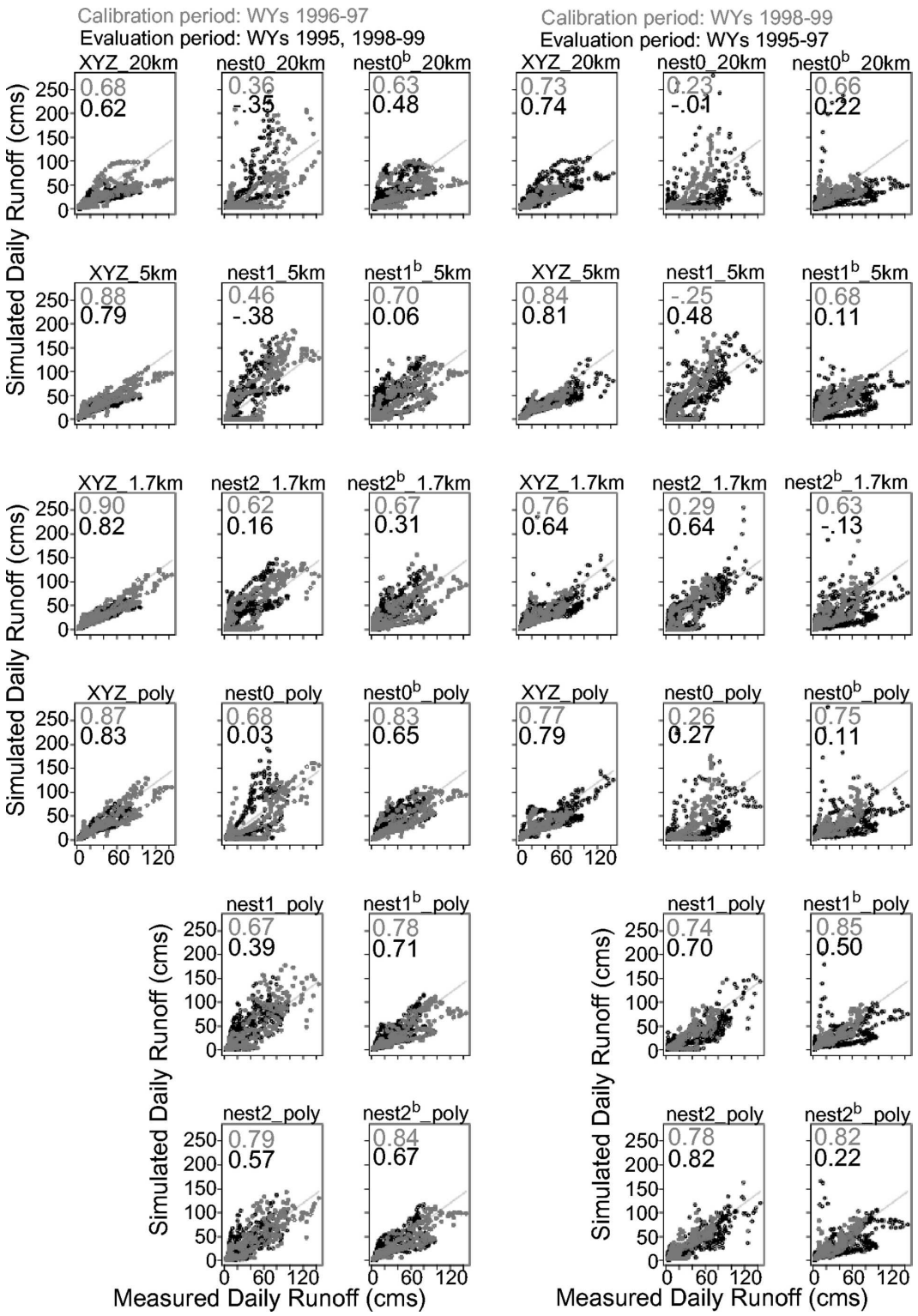

FIG. 14. Measured vs simulated daily runoff from the 16 PRMS simulations and the two calibration (gray)/evaluation (black) periods. Gray line indicates the 1:1 measured daily runoff line. Text in plots indicates the Nash–Sutcliffe goodness-of-fit statistic values for the calibration (gray) and evaluation (black) periods.

should not be expected to correct larger-scale biases produced by the driving (coarser resolution) domain. The finer-scale simulations thus face two areas of improvement: 1) reduction of larger-scale error from the parent simulation, and 2) reduction of local errors that may be produced by the local parameterizations of the boundary layer and surface processes.

The distributed capabilities of PRMS are provided by partitioning the Yampa River basin into hydrologic response units (HRUs). In addition to the classic polygon method of HRU definition, HRUs for PRMS were defined from the three MM5 experiments. This resulted in 16 datasets (see Table 1 for descriptions) tested in PRMS using a multiobjective, stepwise automated calibration procedure.

PRMS was calibrated using each of the 16 input datasets with the same technique to avoid biasing one data input over another. This was an important component of this study: to treat the MM5 output the same as the climate station data. Independent calibration of each dataset avoids biasing one data input over another. Calibration datasets were developed for four PRMS model outputs: 1) solar radiation, 2) potential evapotranspiration (PET), 3) annual water balance, and 4) daily runoff components. Two separate calibration runs of 2 yr were performed for each input dataset: 1) two wet water years (WYs 1998–99) and 2) two dry water years (WYs 1996–97).

Results comparing PRMS output using polygon HRUs and grid-based HRUs generally show an increase in accuracy as resolution increases. Results comparing PRMS output when calibrating using wet versus dry water years show that calibration using wet years generally gives better evaluation results. The multiobjective, stepwise procedure gives the user a higher level of knowledge on how well the intermediate states of PRMS are being reproduced. Analysis of results for each step in the calibration indicates that PRMS is able to simulate solar radiation and PET accurately on a basin mean monthly basis, the annual water balance, and the daily runoff components (groundwater, peak, and daily flows). Comparisons of MMS- and xyz-based PRMS simulations show, for each step of the calibration process, the best overall results for the xyz-based simulations.

An interesting result from this study is that increased horizontal resolution did not markedly improve the accuracy of the MM5 simulations. Because a given MM5 simulation can be viewed as a single (stochastic) realization of seasonal climate, it may be a better use of computer resources to perform MM5 simulations with multiple ensemble members at a coarse horizontal resolution rather than with a deterministic run (a single ensemble member) at a fine horizontal resolution. This probabilistic approach to seasonal climate simulation is consistent with the large uncertainties in seasonal climate forecasts. There is clearly a trade-off between horizontal resolution and ensemble size, and rigorous evaluation of the benefits of each will help guide future regional climate model simulations.

The high-resolution land–atmosphere MM5 simulations introduce the possibility of using the hydrologic storages and fluxes directly from MM5. If this were feasible, then hydrologic simulations could be performed within the atmospheric modeling framework, and there would be no need for a separate hydrologic model. However, this paper indicates that there are large biases in MM5 simulations of near-surface meteorology (precipitation, temperature) that can profoundly affect simulations of land surface storages and fluxes (snowpack, soil moisture, and runoff). Until MM5 biases can be removed, or significantly reduced, there will be a need for offline land surface model simulations of hydrologic processes.

In conclusion, a one-way coupling of an atmospheric and a hydrologic model does not yield runoff simulations that are as accurate as those produced using only climate station data in a hydrologic model. To use fine-resolution atmospheric model output for hydrologic modeling, inaccuracies in the atmospheric model must be addressed. To use MM5 output in hydrologic model simulations at the basin scale, research in the areas of bias identification and removal in the MM5 simulations of local climate are warranted.

REFERENCES

Anderson, J. R., E. E. Hardy, J. T. Roach, and R. E. Witmer, 1976: A land use land cover classification system for use with remote sensor data. U.S. Geological Survey Professional Paper 964, 28 pp.

Benjamin, S. G., and Coauthors, 2004: An hourly assimilation–forecast cycle. The RVC. *Mon. Wea. Rev.,* **132,** 495–518.

Benoit, R., P. Pellerin, N. Kouwen, H. Ritchie, N. Donaldson, P. Joe, and E. D. Soulis, 2000: Toward the use of coupled atmospheric and hydrologic models at regional scale. *Mon. Wea. Rev.,* **128,** 1681–1706.

Blackadar, A. K., 1976: Modeling the nocturnal boundary layer. Preprints, *Third Symp. on Atmospheric Turbulence and Air Quality,* Raleigh, NC, Amer. Meteor. Soc., 46–49.

——, 1979: High resolution models of the planetary boundary layer. *Advances in Environmental Science and Engineering,* Vol. 1, J. R. Pfafflin and E. N. Ziegler, Eds., Gordon and Briech Scientific Publishing, 50–85.

Burk, S. D., and W. T. Thompson, 1989: A vertically nested regional numerical weather prediction model with second-order closure physics. *Mon. Wea. Rev.,* **117,** 2305–2324.

Duan, Q., S. Sorooshian, and V. K. Gupta, 1992: Effective and efficient global optimization for conceptual rainfall-runoff models. *Water Resour. Res.,* **28,** 1015–1031.

——, V. K. Gupta, and S. Sorooshian, 1993: A shuffled complex evolution approach for effective and efficient global minimization. *J. Opt. Theory Appl.,* **76,** 501–521.

——, S. Sorooshian, and V. K. Gupta, 1994: Optimal use of the SCE-UA global optimization method for calibrating watershed models. *J. Hydrol.,* **158,** 265–284.

Dudhia, J., 1989: Numerical study of convection observed during the winter monsoon experiment using a mesoscale two-dimensional model. *J. Atmos. Sci.,* **46,** 3077–3107.

Eischeid, J. K., P. A. Pasteris, H. F. Diaz, M. S. Plantico, and N. J. Lott, 2000: Creating a serially complete, national daily time series of temperature and precipitation for the western United States. *J. Appl. Meteor.,* **39,** 1580–1591.

Farnsworth, R. K., E. S. Thompson, and E. L. Peck, 1982: Evaporation atlas for the contiguous 48 United States. NOAA Tech. Rep. NWS 33, 26 pp.

Grell, G. A., and D. Dévényi, 2002: A generalized approach to parameterizing convection combining ensemble and data assimilation techniques. *Geophys. Res. Lett.,* **29,** 1693, doi:10.1029/2002GL01531.

——, J. Dudhia, and D. R. Stauffer, 1995: A description of the fifth-generation Penn State/NCAR Mesoscale Model (MM5). NCAR Tech. Rep. NCAR/TN-398+STR, 122 pp.

——, L. Schade, R. Knoche, A. Pfeiffer, and J. Egger, 2000: Nonhydrostatic climate simulations of precipitation over complex terrain. *J. Geophys. Res.,* **105** (D24), 29 595–29 608.

Hay, L. E., and M. P. Clark, 2003: Use of statistically and dynamically downscaled atmospheric model output for hydrologic simulations in three mountainous basins in the western United States. *J. Hydrol.,* **282,** 56–75.

——, R. L. Wilby, and G. H. Leavesley, 2000: A comparison of delta change and downscaled GCM scenarios for three mountainous basins in the United States. *J. Amer. Water Resour. Assoc.,* **36,** 387–397.

——, M. P. Clark, R. L. Wilby, W. J. Gutowski, G. H. Leavesley, Z. Pan, R. W. Arritt, and E. S. Takle, 2002: Use of regional climate model output for hydrologic simulations. *J. Hydrometeor.,* **3,** 571–590.

——, G. H. Leavesley, M. P. Clark, S. L. Markstrom, R. J. Viger, and M. Umemoto, 2006: Step-wise, multiple-objective calibration of a hydrologic model for a snowmelt-dominated basin. *J. Amer. Water Resour. Assoc.,* in press.

Hogue, T. S., S. Sorooshian, H. V. Gupta, A. Holz, and D. Braatz, 2000: A multi-step automatic calibration scheme for river forecasting models. *J. Hydrometeor.,* **1,** 524–542.

Kalnay, E., and Coauthors, 1996: The NCEP/NCAR 40-Year Reanalysis Project. *Bull. Amer. Meteor. Soc.,* **77,** 437–471.

Kuczera, G., 1997: Efficient subspace probabilistic parameter optimization for catchment models. *Water Resour. Res.,* **33,** 177–185.

Leavesley, G. H., and L. G. Stannard, 1995: The precipitation-runoff modeling system-PRMS. *Computer Models of Watershed Hydrology,* V. P Singh, Ed., Water Resources Publications, 281–310.

——, R. W. Lichty, B. M. Troutman, and L. G. Saindon, 1983: Precipitation-runoff modeling system: User's manual. U.S. Geological Survey Water Resources Investigations Rep. 83-4238, 207 pp.

Leung, L. R., and Y. Qian, 2003: The sensitivity of precipitation and snowpack simulations to model resolution via nesting in regions of complex terrain. *J. Hydrometeor.,* **4,** 1025–1043.

Lin, C. A., L. Wen, M. Beland, and D. Chaumont, 2002: A coupled atmospheric-hydrological modeling study of the 1996 Ha! Ha! River basin flash flood in Quebec, Canada. *Geophys. Res. Lett.,* **29,** 1026, doi:10.1029/2001GL013827.

Madsen, H., 2003: Parameter estimation in distributed hydrological catchment modelling using automatic calibration with multiple objectives. *Adv. Water Resour.,* **26,** 205–216.

McCarthy, J. J., O. F. Canziani, N. A. Leary, D. J. Dokken, and K. S. White, Eds., 2001: *Climate Change 2001: Impacts, Adaptation, Vulnerability*. Cambridge University Press, 1032 pp.

Mlawer, E. J., S. J. Taubman, P. D. Brown, M. J. Iacono, and S. A. Clough, 1997: Radiative transfer for inhomogeneous atmospheres: RRTM, a validated correlated-k model for the longwave. *J. Geophys. Res.,* **102,** 16 663–16 682.

Nash, J. E., and J. V. Sutcliffe, 1970: River flow forecasting through conceptual models part I—A discussion of principles. *J. Hydrol.,* **10,** 282–290.

Panofsky, H. A., and G. W. Brier, 1968: *Some Applications of Statistics to Meteorology*. The Pennsylvania State University Press, 224 pp.

Phillips, T. J., 1995: Documentation of the AMIP models on the World Wide Web. Lawrence Livermore Laboratory PCMDI Rep. 24, 14 pp.

Reek, T., S. R. Doty, and T. W. Owen, 1992: A deterministic approach to the validation of historical daily temperature and precipitation data from the cooperative network. *Bull. Amer. Meteor. Soc.,* **73,** 753–762.

Reisner, J., R. J. Rasmussen, and R. T. Bruintjes, 1998: Explicit forecasting of supercooled liquid water in winter storms using the MM5 mesoscale model. *Quart. J. Roy. Meteor. Soc.,* **124,** 1071–1107.

Seuffert, G., P. Gross, C. Simmer, and E. F. Wood, 2002: The influence of hydrologic modelling on the predicted local weather: Two-way coupling of a mesoscale land surface model and a land surface hydrologic model. *J. Hydrometeor.,* **3,** 505–523.

Sloto, R. A., and M. Y. Crouse, 1996: HYSEP: A computer program for streamflow hydrograph separation and analysis. U.S. Geological Survey Water-Resources Investigations Rep. 96-4040, 46 pp.

Smirnova, T. G., J. M. Brown, S. G. Benjamin, and K. Dongsoo, 2000: Parameterization of cold-season processes in the MAPS land-surface scheme. *J. Geophys. Res.,* **105,** 4077–4086.

U.S. Department of Agriculture, 1994: State Soil Geographic (STATSGO) database—Data use information. Natural Resources Conservation Service, Miscellaneous Publication 1492, 107 pp.

Viger, R. J., S. L. Markstrom, and G. H. Leavesley, 1998: The GIS Weasel—An interface for the treatment of spatial information used in watershed modeling and water resource management. *Proc. of the First Federal Interagency Hydrologic Modeling Conf.,* Vol II, Las Vegas, NV, Subcommittee on Hydrology of the Interagency Advisory Committee on Water Data, 73–80.

Vrugt, J. A., W. Bouten, H. V. Gupta, and S. Sorooshian, 2003: Toward improved identifiability of hydrologic model parameters: The information content of experimental data. *Water Resour. Res.,* **38,** 1312, doi:10.1029/2001WR001118.

Westrick, K. J., and C. F. Mass, 2001: An evaluation of a high-resolution hydrometeorological modeling system for predic-

tion of a cold-season flood event in a coastal mountainous watershed. *J. Hydrometeor.,* **2,** 161–180.

——, P. Storck, and C. F. Mass, 2002: Description and evaluation of a hydrometeorological forecast system for mountainous watersheds. *Wea. Forecasting,* **17,** 250–262.

Wilby, R. L., L. E. Hay, and G. H. Leavesley, 1999: A comparison of downscaled and raw GCM output: Implications for climate change scenarios in the San Juan River basin, Colorado. *J. Hydrol.,* **225,** 67–91.

Wilks, D. S., 1995: *Statistical Methods in the Atmospheric Sciences: An Introduction*. Academic Press, 467 pp.

Wood, A. W., E. P. Maurer, A. Kumar, and D. P. Lettenmaier, 2002: Long-range experimental hydrological forecasting for the eastern United States. *J. Geophys. Res.,* **107,** 4429, doi:10.1029/2001JD000659.

Yapo, P. O., H. V. Gupta, and S. Sorooshian, 1996: Automatic calibration of conceptual rainfall-runoff models: Sensitivity to calibration data. *J. Hydrol.,* **181,** 23–48.